The Company of Biologists

RESEARCH ARTICLE

A fragment of adhesion molecule L1 is imported into mitochondria, and regulates mitochondrial metabolism and trafficking

Kristina Kraus[1], Ralf Kleene[1], Ingke Braren[2], Gabriele Loers[1], David Lutz[3] and Melitta Schachner[4,5,*]

ABSTRACT

The cell adhesion molecule L1 (also known as L1CAM) plays important roles in the mammalian nervous system under physiological and pathological conditions. We have previously reported that proteolytic cleavage of L1 by myelin basic protein leads to the generation of a 70 kDa transmembrane L1 fragment (L1-70) that promotes neuronal migration and neuritogenesis. Here, we provide evidence that L1-70 is imported from the cytoplasm into mitochondria. Genetic ablation of L1, inhibition of mitochondrial import of L1-70 or prevention of myelin basic protein-mediated generation of L1-70 all lead to reduced mitochondrial complex I activity, and impaired mitochondrial membrane potential, fusion, fission and motility, as well as increased retrograde transport. We identified NADH dehydrogenase ubiquinone flavoprotein 2 as a binding partner for L1, suggesting that L1-70 interacts with this complex I subunit to regulate complex I activity. The results of our study provide insights into novel functions of L1 in mitochondrial metabolism and cellular dynamics. These functions are likely to ameliorate the consequences of acute nervous system injuries and chronic neurodegenerative diseases.

KEY WORDS: L1CAM, Mitochondria, Mitochondrial metabolism, Respiratory chain, Complex I

INTRODUCTION

The cell adhesion molecule L1 (also known as L1CAM) plays crucial roles in a number of cellular processes during development of the central and peripheral nervous systems. It is involved in regulation of cell proliferation and migration, and participates in neuritogenesis, fasciculation of axons, myelination, synaptogenesis, synaptic plasticity and regeneration after acute and during chronic neural impairments (for reviews, see Kamiguchi et al., 1998; Hortsch, 2000; Loers and Schachner, 2007; Maness and Schachner, 2007; Schmid and Maness, 2008; Hortsch et al., 2014; Sytnyk et al., 2017). In the mouse, genetic ablation of L1 leads to malformation of the brain and of other L1-expressing organs, such as the kidney and

[1]Zentrum für Molekulare Neurobiologie, Universitätsklinikum Hamburg-Eppendorf, Falkenried 94, 20251 Hamburg, Germany. [2]Vector Core Unit, Institut für Experimentelle Pharmakologie und Toxikologie, Universitätsklinikum Hamburg-Eppendorf, Martinistr. 52, 20246 Hamburg, Germany. [3]Institut für Strukturelle Neurobiologie, Universitätsklinikum Hamburg-Eppendorf, Falkenried 94, 20251 Hamburg, Germany. [4]Keck Center for Collaborative Neuroscience and Department of Cell Biology and Neuroscience, Rutgers University, 604 Allison Road, Piscataway, NJ 08854, USA. [5]Center for Neuroscience, Shantou University Medical College, 22 Xin Ling Road, Shantou, Guangdong 515041, China.

*Author for correspondence (schachner@stu.edu.cn)

K.K., 0000-0002-4237-7725; R.K., 0000-0002-5935-5266; I.B., 0000-0002-5676-9850; G.L., 0000-0003-1851-562X; D.L., 0000-0002-5449-294X; M.S., 0000-0002-3316-0778

enteric nervous system (Dahme et al., 1997; Debiec et al., 2002; Anderson et al., 2006; Wallace et al., 2011). In humans, L1 is associated with neural disorders, such as L1 syndrome, which is characterized by hydrocephalus, mental retardation, aphasia, adducted thumbs and motor dysfunctions, such as ataxia, paraplegia and shuffling gate. L1 is also associated with the fetal alcohol syndrome, Hirschsprung's disease, schizophrenia and Alzheimer's disease (Poltorak et al., 1995; Kurumaji et al., 2001; Strekalova et al., 2006; Wakabayashi et al., 2008; for reviews, see Maness and Schachner, 2007; Schäfer and Altevogt, 2010; Sytnyk et al., 2017).

Proteolytic cleavage of L1 has been observed to be important for the dynamic functions of L1. We have shown that the involvement of L1 in neuritogenesis and neuronal migration depends on its proteolytic cleavage by the serine protease activity of myelin basic protein (MBP) which cleaves L1 in its extracellular domain at Arg_{687} (Lutz et al., 2014a). MBP-mediated proteolytic processing of L1 is implicated in many functions of L1-expressing neurons and Schwann cells: it not only promotes neurite outgrowth and neuronal cell migration, but also neuronal survival, Schwann cell proliferation, migration and process formation, as well as myelination of axons by Schwann cells *in vitro*. In mouse models, L1 promotes axonal regrowth/sprouting, remyelination and improves functional recovery after acute trauma and under neurodegenerative conditions (Roonprapunt et al., 2003; Barbin et al., 2004; Chen et al., 2007; Lavdas et al., 2010; Cui et al., 2011; Xu et al., 2011; Lutz et al., 2012, 2014a,b, 2016).

MBP-mediated cleavage of L1 at the plasma membrane leads to the generation of a 70 kDa transmembrane L1 fragment (L1-70) that comprises part of the first fibronectin type III homologous repeat, the whole second, third, fourth and fifth fibronectin type III homologous repeat, and the transmembrane and the intracellular domains. L1-70 is transferred to endosomes, released from the endosomes into the cytoplasm and then imported from there into the nucleus (Lutz et al., 2012). In the present study, we identified MBP-generated L1-70 in mitochondria from murine brains.

Mitochondria are the powerhouse of all eukaryotic cells and are particularly important for homeostasis of the energy-demanding neural cells. Mitochondria generate energy through the oxidative phosphorylation machinery, consisting of five enzyme complexes embedded in the inner mitochondrial membrane. These complexes transfer the redox energy of the reduced nicotinamide adenine dinucleotide (NADH) and flavin adenine dinucleotide ($FADH_2$) to oxygen and thereby generate a proton concentration gradient across the inner membrane and synthesize adenosine-5′-triphosphate (ATP) using the electrochemical energy of this gradient. Complex I mediates the oxidation of NADH to NAD^+ and the concomitant reduction of ubiquinone to ubiquinol leading to the transfer of four protons from the mitochondrial matrix to the intermembrane space. Complex II catalyzes the oxidation of $FADH_2$ to FAD and the concomitant reduction of ubiquinone to ubiquinol. Complex III

1

mediates the reduction of cytochrome c by the oxidation of ubiquinol leading to the translocation of four protons from the mitochondrial matrix to the intermembrane space. Complex IV catalyzes the transfer of electrons from reduced cytochrome c to O_2 leading to the translocation of four protons across the inner mitochondrial membrane. The flux of protons from the intermembrane space to the mitochondrial matrix through complex V leads to the production of ATP.

Most of the mitochondrial proteins are encoded by nuclear DNA and imported into mitochondria after their synthesis in the cytoplasm. The import is mediated by protein complexes in the outer and inner membrane (for reviews, see Endo and Yamano, 2010; Schmidt et al., 2010; Becker et al., 2012; Ferramosca and Zara, 2013). The majority of mitochondrial proteins have well-characterized N-terminal mitochondria-targeting sequences (MTSs), which are cleaved off after or during import. Several other proteins lack a cleavable N-terminal MTS and contain less-defined internal targeting signals.

Mitochondria are highly dynamic organelles: they undergo fission and fusion and move bidirectionally (for reviews, see Chen and Chan, 2009, Oliveira, 2011). These dynamic processes depend on the mitochondrial membrane potential, which is established by the proton gradient across the inner membrane. Impaired generation and maintenance of the membrane potential reduces mitochondrial biogenesis due to defective protein import, and inhibits fusion of mitochondria. Thus, fragmented mitochondria that cannot re-establish their membrane potential after fission are not competent for fusion. Moreover, changes in the membrane potential have been associated with alterations in the direction of mitochondrial trafficking and motility (for a review, see Oliveira, 2011). In addition, defects in fusion or fission decrease mitochondrial motility (for a review, see Chen and Chan, 2009).

In the present study, we show that MBP-generated L1-70 is imported into mitochondria, where it plays important roles in regulation of complex I activity and generation of the mitochondrial membrane potential. Moreover, L1-70 is also involved in controlling mitochondrial fusion, fission, motility and trafficking.

RESULTS
A L1 fragment is imported into mouse brain mitochondria
We have previously shown that L1 interacts with glyceraldehyde 3-phosphate dehydrogenase (GAPDH) and with the adenine nucleotide translocator 1 and 2 (ANT1 and ANT2; also known as SLC25A4 and SLC25A5, respectively) at the cell surface of neurons via binding sites in its extracellular domain (Makhina et al., 2009; Loers et al., 2012). Since GAPDH, as well as ANT1 and ANT2, are mitochondrial proteins with important mitochondrial functions, and since the transmembrane L1-70 fragment, which contains part of the extracellular domain, can be detected in the cytoplasm (Lutz et al., 2012), we tested whether L1-70 is imported from the cytoplasm into mitochondria to interact with GAPDH, ANT1 and/or ANT2. To this aim, mitochondria were isolated from brains of wild-type and L1-deficient mice and subjected to western blot analysis with a rabbit antibody against the intracellular L1 domain. In parallel, mitochondria were subjected to immunoprecipitation with mouse antibody against the intracellular L1 domain, and probed by means of western blot analysis with a rabbit antibody against the intracellular L1 domain. An L1-immunopositive band of ∼70 kDa was observed in wild-type mitochondria, but not in L1-deficient mitochondria (Fig. 1A). This band, hereafter referred to as L1-70, was also detected in L1 immunoprecipitates from wild-type mitochondria, but not in

immunoprecipitates using a non-immune control antibody (Fig. 1B). No L1-immunopositive band of ∼200 kDa corresponding to the full-length L1 was detectable in wild-type mitochondria (Fig. 1A,B). To check the purity of the mitochondrial fraction, it was tested for the presence of marker proteins for mitochondria, endosomes, endoplasmic reticulum, cytoplasm and nuclei. Total brain homogenate and fractions enriched in cytoplasm, nuclei, endosomes or endoplasmic reticulum served as controls. In the total brain homogenate, no or hardly detectable levels of the marker proteins were seen (Fig. 1C). The mitochondrial proteins VDAC1 and NdufV3 were only detectable in the mitochondrial fraction, but not in the other fractions (Fig. 1C). In contrast, the nuclear protein histone H3 was exclusively found in the nuclear fraction (Fig. 1C). Calreticulin, a marker protein of the endoplasmic reticulum, was predominantly detected in the microsomal 100,000 g pellet fraction, which is enriched in endosomes and endoplasmic reticulum (Fig. 1C). The very small levels of calreticulin detectable in the mitochondrial fraction (Fig. 1C) likely derive from mitochondria-associated membranes, which represent a specialized region of the endoplasmic reticulum (for a review, see Vance, 2014). The cytoplasmic protein RhoA was observed in the cytoplasmic 100,000 g supernatant fraction, but not in mitochondria (Fig. 1C). Rab7, a marker of late endosomes, and EEA1, a marker of early endosomes were present in the cytoplasmic and/or microsomal fraction (Fig. 1C). These results show that the mitochondrial fraction is highly enriched in mitochondria, depleted in endoplasmic reticulum and devoid of endosomal, cytoplasmic and nuclear proteins.

Probing the subcellular fractions for the presence of full-length L1 and L1-70 showed full-length L1 and L1-70 in total brain homogenate, as well as cytoplasmic and microsomal fractions, and L1-70, but not full-length L1, in mitochondrial and nuclear fractions (Fig. 1C).

Interestingly, L1-70 was also found in GAPDH immunoprecipitates from wild-type mitochondria, but not in GAPDH immunoprecipitates from L1-deficient mitochondria or in non-immune control immunoprecipitates from wild-type mitochondria (Fig. 1D). In contrast, no L1-70 was found in immunoprecipitates obtained with different antibodies against ANT1 and ANT2 (data not shown). These results suggest that L1-70 is imported into mitochondria where it interacts with GAPDH, but not with ANT1 and ANT2.

To test whether L1-70 is imported from the cytoplasm into the mitochondria, an in vitro import assay with a cytoplasmic fraction from brains of wild-type mice and mitochondria from brains of L1-deficient mice was performed. After incubation of L1-lacking mitochondria with L1-containing cytoplasm and re-isolation of mitochondria, L1-70 could be detected in the re-isolated mitochondria (Fig. 1E). The L1 fragment was also seen after treatment of re-isolated mitochondria with trypsin, whereas it was no more detectable in mitochondria after trypsin treatment in the presence of the membrane-solubilizing detergent Triton X-100 (Fig. 1E). These results indicate that L1-70 is imported from the cytoplasm into the L1-lacking mitochondria, where it is protected against digestion by trypsin.

To characterize at the molecular level the mechanisms underlying mitochondrial import of L1-70, we analyzed whether the import of L1-70 involves the translocase of the outer membrane (TOM) complex. To this aim, we analyzed whether the import of the fragment was blocked by an antibody against TOM70, which acts as a receptor for proteins that do not possess a cleavable N-terminal MTS but carry internal targeting signals. In parallel, an antibody
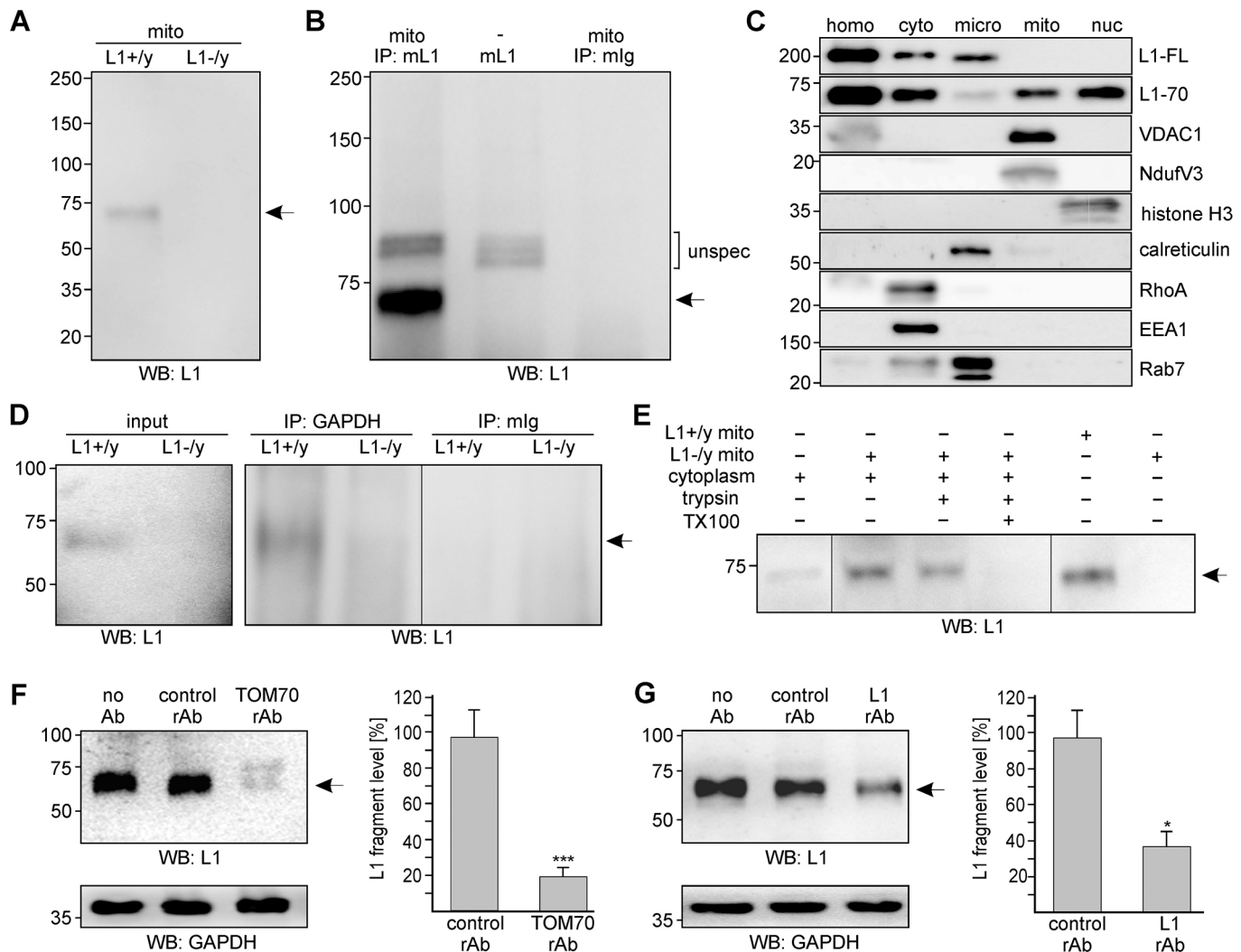
Fig. 1. L1-70 is imported into mitochondria. (A) L1-70 is detected by western blot (WB) analysis in brain mitochondria (mito) from wild-type (L1+/y) mice, but not in brain mitochondria from L1-deficient (L1−/y) mice. (B) L1-70 is found in immunoprecipitates with mouse anti-L1 antibody (IP: mL1) from brain mitochondria (mito) of wild-type mice, but not in immunoprecipitates obtained with control mouse antibody (IP: mIg). The bracket indicates unspecific bands recognized by the mouse anti-L1 antibody (mL1). (C) Western blots with antibodies against L1, VDAC1, NdufV3, histone H3, calreticulin, RhoA, Rab7 or EEA1 using brain homogenate (homo) and cytoplasmic (cyto), nuclear (nuc), mitochondrial (mito) and microsomal (micro) fractions. L1-FL, full-length L1. (D) L1-70 is found in GAPDH immunoprecipitates (IP: GAPDH) and input from mitochondria of wild-type (L1+/y) mice, but it was neither detectable in GAPDH immunoprecipitates (IP: GAPDH) nor in input from mitochondria of L1-deficient (L1−/y) mice or in control immunoprecipitates (IP: mIg) from mitochondria of wild-type (L1+/y) mice. (E) L1-70 is present in mitochondria after incubation of brain mitochondria from L1-deficient (L1−/y) mice with cytoplasm of brains from wild-type (L1+/y) mice in the absence or presence of trypsin, while it is not detectable after incubation in the concomitant presence of trypsin and Triton X-100 (TX100). (F,G) Levels of L1-70 are decreased after incubation of L1-deficient brain mitochondria with wild-type brain cytoplasm in the presence of rabbit anti-TOM70 (F) or -L1 (G) antibody, while the levels are not altered after incubation in the presence of control rabbit antibodies (rAb). Results are mean±s.e.m. from five independent experiments and statistical differences are shown for the L1-70 level relative to the control without antibody treatment (set to 100%) (*P<0.01; ***P<0.001; one-way ANOVA with Holm–Sidak multiple comparison test). In A–G, representative western blots with rabbit anti-L1 antibody (A,B,D–G), anti-GAPDH antibody (F,G), anti-L1 antibody C-2 recognizing full-length L1 (L1-FL) and L1-70 (C), or with antibodies against VDAC1, NdufV3, histone H3, calreticulin, RhoA, Rab7 or EEA1 (C) out of four (A,B,D,E), three (C) or five (F,G) experiments are shown. L1-70 is indicated by an arrow. Lanes not adjacent to each other but derived from the same blot are indicated by a vertical line.

against an extracellular membrane-proximal epitope in L1 was used to specifically block the import of L1-70, and a non-immune control antibody served as negative control. The L1 and TOM70 antibodies inhibited the import of L1-70 from the cytoplasm into the L1-lacking mitochondria, while the non-immune control antibodies did not block this import (Fig. 1F,G). This result indicates that L1-70 is imported into mitochondria via the TOM import machinery.

To verify by a different technique that L1 is present in mitochondria, immunoelectron microscopy of sections from cerebella of wild-type and L1-deficient mice was performed. The images showed immunogold nanoparticle clusters immunoreactive

for L1 not only at the surface but also inside of mitochondria (Fig. 2).

L1-70 regulates complex I activity and mitochondrial membrane potential

Mitochondria from wild-type and L1-deficient mice were examined to clarify whether absence of L1-70 affects mitochondrial metabolism. Since the respiratory chain is responsible for generating a proton gradient, which establishes the mitochondrial membrane potential across the inner membrane and drives the ATP production by complex V, we determined the activities of
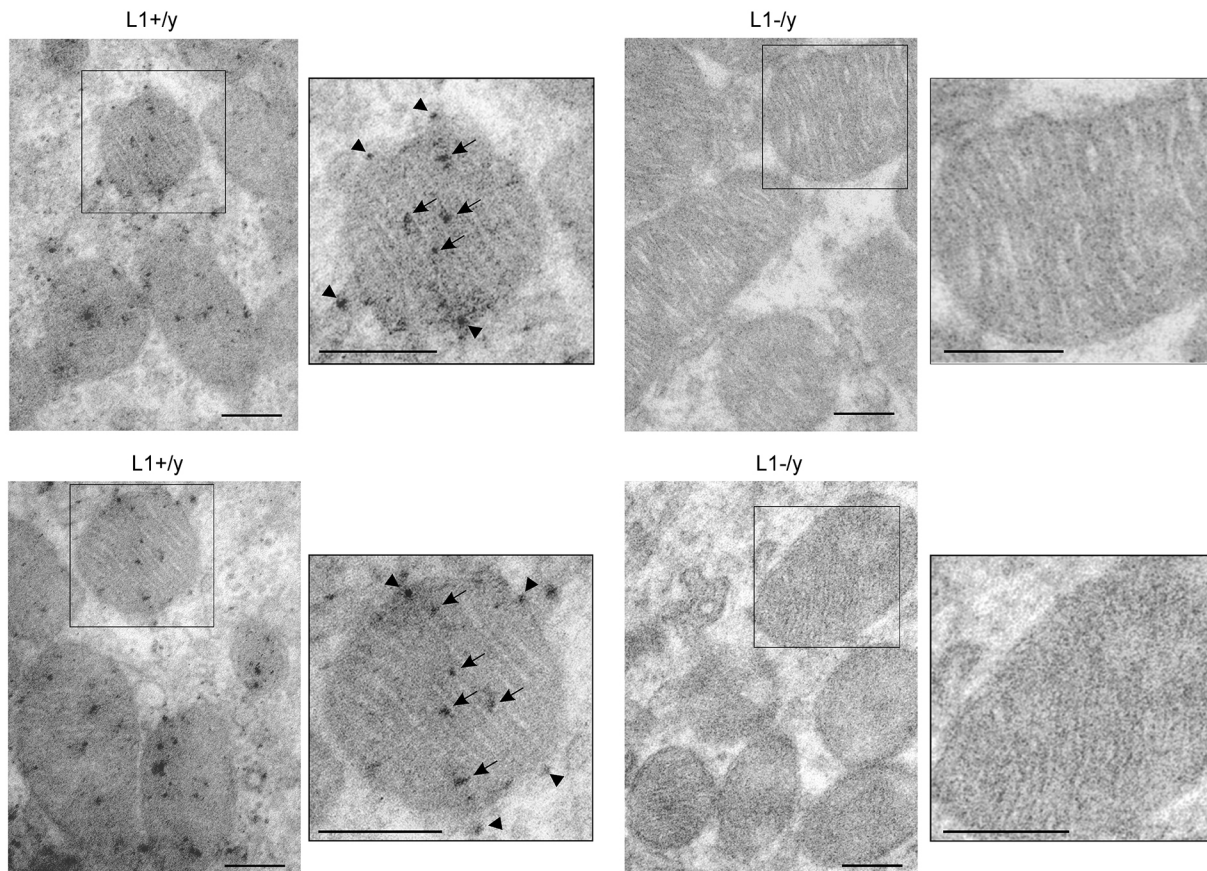
Fig. 2. Localization of L1 in mitochondria by immunoelectron microscopy. Tissue sections from cerebella of wild-type mice (L1+/y) and L1-deficient littermates (L1−/y) were subjected to immunoelectron microscopy using the anti-L1 antibody H-200, which recognizes an extracellular membrane-proximal epitope. L1-reactive immunogold nanoparticles are found in mitochondria of wild-type cerebellar granule cells. No L1-reactive immunogold nanoparticles were detectable in mitochondria of L1-deficient cerebellar granule cells. Rectangles show single mitochondria at high magnification; arrows indicate immunogold nanoparticle clusters within mitochondria and arrowheads indicate immunogold nanoparticle clusters at the mitochondrial surface. Two representative images from two mice are shown. Note that L1 is localized at the surface of mitochondria and inside mitochondria. Scale bars: 200 nm.

complex V and complex I, which contribute to the generation of the proton gradient. Relative to the activity in wild-type mitochondria, ATP synthase activity was slightly, but not significantly, increased in L1-deficient mitochondria (100±39% versus 113±42%; mean± s.e.m.; n=6 animals), while complex I activity in L1-deficient mitochondria was lower than that in wild-type littermate mitochondria (Fig. 3A). This result indicates that L1 regulates complex I activity and suggests that this activity depends on the import of L1-70.

To analyze whether members of the immunoglobulin superfamily, which are functionally and structurally related to L1, also regulate complex I activity, complex I activities were determined in mitochondria from CHL1- and NCAM (also known as NCAM1)-deficient mice. Complex I activities in mitochondria from CHL1-deficient and NCAM-deficient mice were similar to the complex I activities of their wild-type littermates (Fig. 3A).

Since complex II, III and IV also contribute to establishing the proton gradient, the activity of these complexes was determined in mitochondria from mice deficient in L1, CHL1 or NCAM. Relative to the wild-type littermate activities, complex II/III and complex IV activities were not changed (Fig. 3B,C).

To confirm that regulation of complex I activity by L1 depends on the import of L1-70 into mitochondria, complex I activity was determined in isolated L1-lacking mitochondria after incubation with cytoplasm from the brains of wild-type mice. After incubation

of L1-lacking mitochondria with L1-containing cytoplasm, complex I activity was increased when compared to mitochondrial activity in the absence of cytoplasm (Fig. 3D). After incubation of mitochondria with cytoplasm in the presence of L1-70 import-blocking anti-TOM70 or -L1 antibodies, complex I activity was not enhanced, but was similar to that of L1-deficient mitochondria incubated in the absence of cytoplasm (Fig. 3D). In the presence of non-immune control antibodies, complex I activity was enhanced (Fig. 3D). These results indicate that import of L1-70 into mitochondria is required for regulating complex I activity.

To investigate whether reduced complex I activity in the absence of L1 impairs the mitochondrial membrane potential, a green fluorescent membrane potential indicator was applied to cultures of wild-type and L1-deficient cerebellar neurons. This indicator accumulates in the form of orange-fluorescent aggregates in mitochondria with intact membrane potential, but does not accumulate in mitochondria with impaired membrane potential. The ratio of orange to green fluorescence intensities determined in wild-type cerebellar neurons was higher than in L1-deficient neurons (Fig. 4A), indicating that L1-deficient mitochondria have a reduced membrane potential relative to wild-type mitochondria.

To analyze whether the generation and mitochondrial import of the MBP-generated L1-70 is responsible for the generation and maintenance of a proper mitochondrial membrane potential, we applied the membrane potential indicator to L1-lacking HEK293
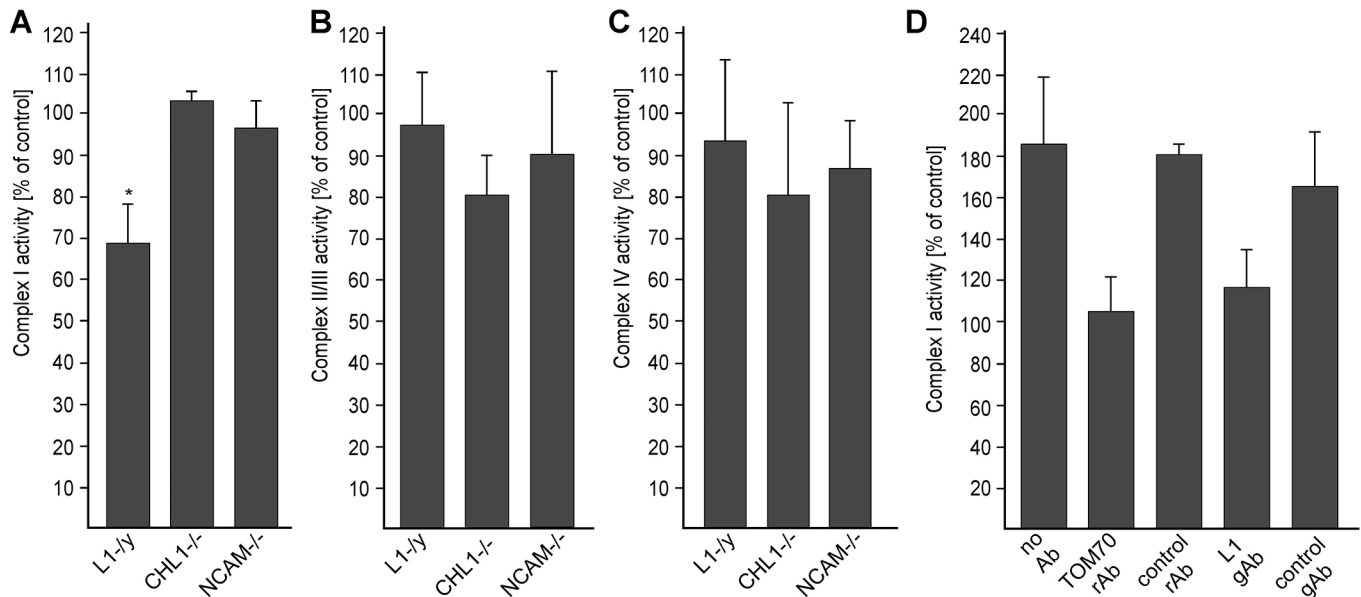
Fig. 3. Complex I activity is impaired in mitochondria from brains of L1-deficient mice. (A–C) Activity of complex I is reduced in mitochondria from brains of L1-deficient (L1–/y) mice relative to the activity in mitochondria from brains of wild-type mice ($n=6$) (set to 100%), while the activity of complex II, III and IV was similar in L1-deficient and wild-type mice ($n=5$) (set to 100%). Activity of complex I, II, III and IV was similar in NCAM- or CHL1-deficient mice relative to wild-type littermates ($n=4$) (set to 100%). Mean±s.e.m. values are shown, and differences between the groups are indicated (*$P<0.05$; two-tailed Student's t-test). (D) Activity of complex I is enhanced in L1-deficient brain mitochondria after incubation with cytoplasm from brains of wild-type mice in the absence of antibodies (no Ab) or presence of control antibodies (control Ab), and in comparison to the activity after incubation in the absence of cytoplasm (set to 100%). Activity of complex I is not enhanced after incubation in presence of anti-TOM70 or -L1 antibody. Mean±s.e.m. values from three independent experiments are shown.

cells after transduction with control adeno-associated virus (AAV) not coding for L1 or with AAV encoding wild-type L1 or the L1 mutant disrupted in the MBP cleavage site. It is important to mention in this context that L1-negative HEK293 cells express MBP, which generates L1-70 upon induction of L1 expression (Lutz et al., 2014a). Cells transduced with wild-type L1 showed a higher ratio of orange to green fluorescence intensity than cells transduced with control AAV (Fig. 4B), indicating that L1-negative HEK293 cells have an impaired membrane potential and that transduced HEK293 cells expressing wild-type L1 have an intact membrane potential. After transduction with the L1 mutant, cells showed a lower ratio of orange to green fluorescence intensity than cells transduced with AAV coding for wild-type L1 or cells transduced with control AAV (Fig. 4B), indicating that the generation of L1-70 and mitochondrial import of L1-70 are crucial for formation and/or maintenance of an intact mitochondrial membrane potential.

Fusion of mitochondria depends on L1-70

Since mitochondria do not fuse with other mitochondria when they have an impaired membrane potential or are unable to establish an intact membrane potential after fission, we examined whether the decreased membrane potential in L1-deficient cerebellar neurons and in L1-negative HEK293 cells is associated with enhanced mitochondrial fragmentation due to impaired fusion. Staining of mitochondria with MitoTracker showed several elongated mitochondria in neurites of wild-type neurons, while no elongated and only a few small round mitochondria were found in the neurites of L1-deficient neurons (Fig. 5A). In HEK293 cells transduced with AAV encoding wild-type L1, the majority of mitochondria showed elongated shapes, whereas predominantly small and round mitochondria were detectable in cells transduced with control AAV or with AAV encoding the L1 mutant (Fig. 5B). Since an elongated shape is indicative of intact fission–fusion cycles and a round shape indicates fragmented mitochondria and impaired

fission and/or fusion of mitochondria, we conclude that absence of L1 or the lack of mitochondrial import of L1-70 results in defects in mitochondrial fission and fusion.

To verify that the fusion of mitochondria depends on the presence of L1-70, HEK293 cells transduced with control AAV or with AAV encoding wild-type or mutant L1 were transfected with the MitoDendra-2 plasmid encoding the mitochondrially localized version of the photo-convertible fluorescent protein Dendra-2. Cells were exposed to a spot of UV light, which converts the fluorescence of MitoDendra-2 from green into red, and the fusion of red-labeled and green-labeled mitochondria near the UV-exposed area was analyzed by determining yellow-labeled spots. Fusion in cells expressing wild-type L1 was more pronounced than in L1-negative cells or L1 mutant-expressing cells (Fig. 5C,D). These results indicate that the fusion of mitochondria depends on L1-70.

L1-70 regulates mitochondrial motility

Since the mitochondrial membrane potential not only affects mitochondrial dynamics, but also affects mitochondrial trafficking (for a review, see Oliveira, 2011), we tested whether the decreased membrane potential in L1-deficient cerebellar neurons affects mitochondrial motility. Indeed, this motility was reduced in L1-deficient neurons at 3 days of culture when compared to that in wild-type neurons (Fig. 6A). Moreover, the motility of mitochondria in wild-type cerebellar neurons was increased after treatment with a function-triggering L1 antibody, which stimulates generation and nuclear import of L1-70 (Lutz et al., 2012) (Fig. 6B), indicating that enhanced L1-70 levels are associated with accelerated motility. Since MBP-deficient shiverer mutant mice are devoid of L1-70, but not of full-length L1 (Lutz et al., 2014a), we used cerebellar neurons from shiverer mice to test whether the motility of mitochondria was reduced in the absence of L1-70. When compared to their wild-type littermates, mitochondria in MBP-deficient L1-70-devoid cerebellar neurons were strongly reduced in motility (Fig. 6C). This
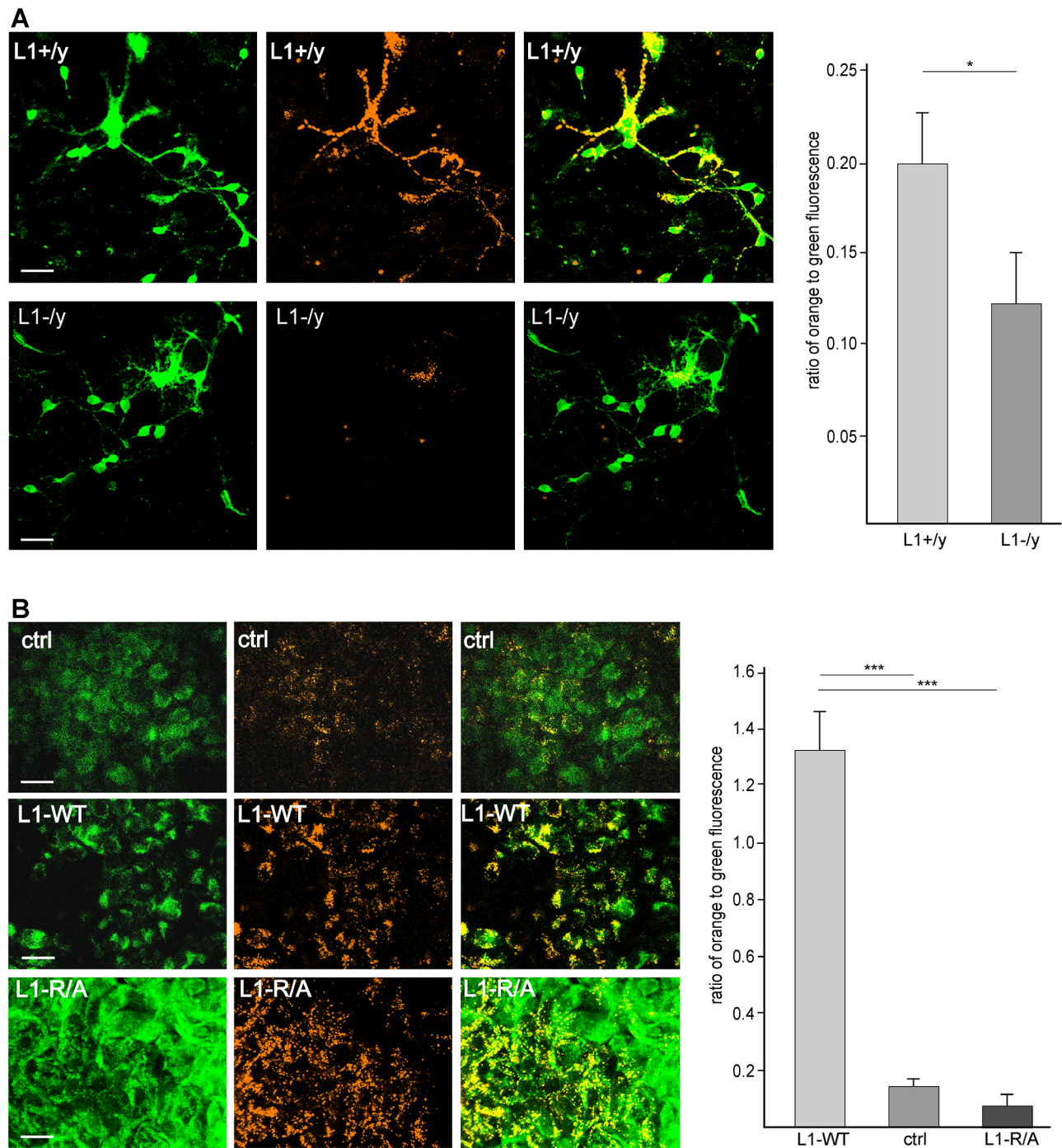
Fig. 4. The mitochondrial membrane potential is impaired in the absence of L1-70. Cerebellar neurons from wild-type (L1+/y) and L1-deficient (L1−/y) mice (A) and HEK293 cells transduced with control AAV or with AAV coding for wild-type L1 (L1-WT) or the L1-R/A mutant (L1-R/A) (B) were incubated with the membrane potential reagent MITO-ID, which shows green fluorescence in the cytoplasm and accumulates as orange-fluorescent aggregates in mitochondria with intact membrane potential. Representative images are shown from two independent experiments. The corrected total cell fluorescence was calculated for the green and orange channel from 17 (A) or 5 (B) images per group and experiment. Determination of the orange to green fluorescence ratio shows that the membrane potential is impaired in L1-deficient neurons (A), in mock-transduced L1-lacking HEK293 cells and in HEK293 cells expressing the L1 mutant (B). Mean±s.e.m. coefficient values from two independent experiments are shown and differences between groups are indicated. *$P<0.05$, one-tailed Student's t-test (A); ***$P<0.001$, one-way ANOVA with Holm–Sidak multiple comparison test (B). Scale bars: 50 µm.

finding was confirmed with cerebellar L1-deficient neurons that were transduced with control AAV or with AAV encoding wild-type L1 or L1 mutant. Motility in neurons expressing AAV encoding wild-type L1 was higher than in L1-deficient neurons transduced with control AAV (Fig. 6D) and reached the values of motility seen in wild-type neurons (Fig. 6A). Mitochondria in neurons expressing

the mutated L1 did not show enhanced motility relative to mitochondria in neurons transduced with control AAV (Fig. 6D) or in L1-deficient neurons (Fig. 6A). These results indicate that mitochondrial motility is affected by L1-70.

Since mitochondria with an intact membrane potential preferentially move anterogradely, and mitochondria with an
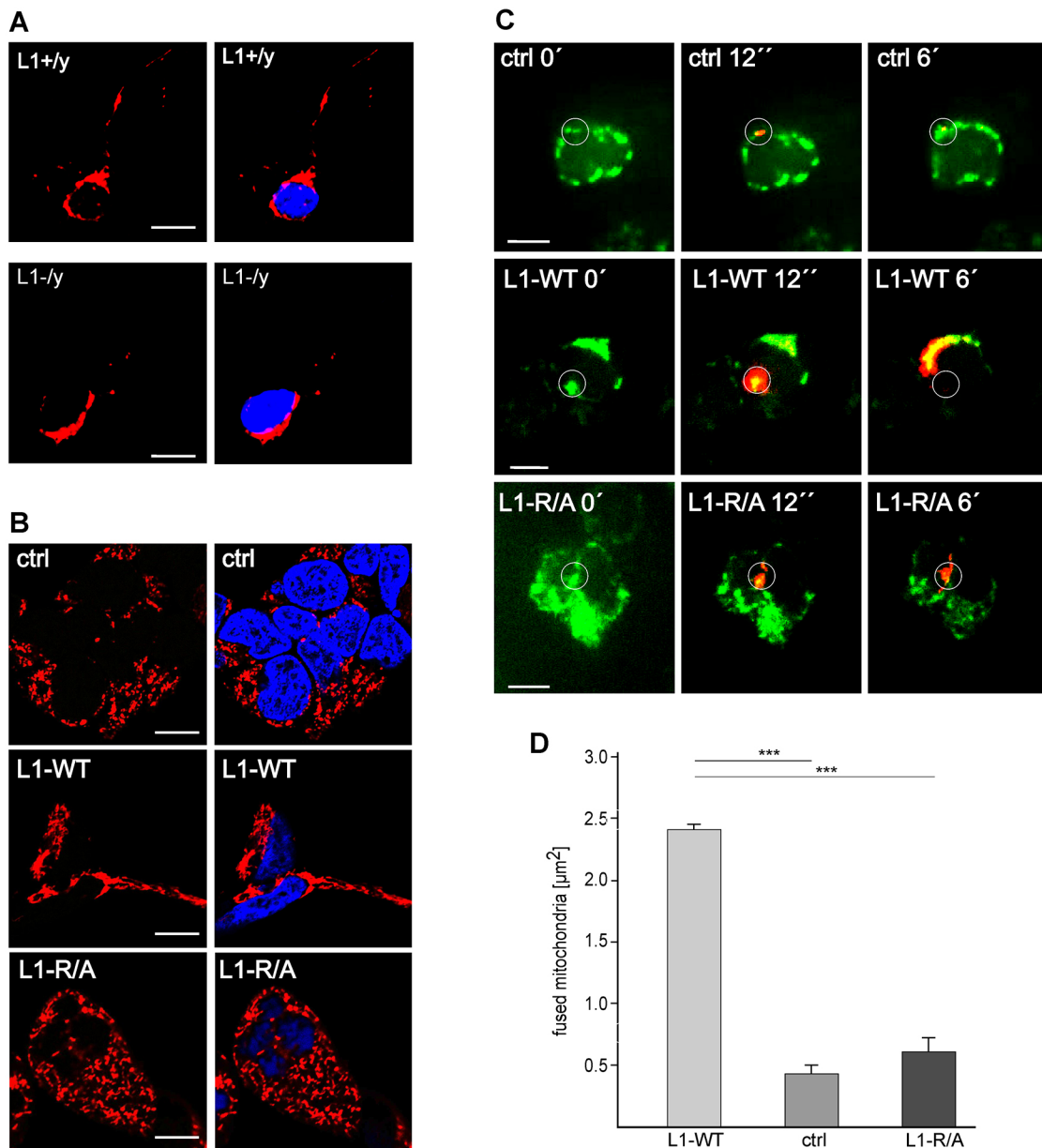
Fig. 5. Fusion of mitochondria is impaired in the absence of L1-70. Labeling of mitochondria with MitoTracker shows elongated mitochondria along neurites of wild-type (L1+/y) neurons (A) and in HEK293 cells transduced with wild-type L1 (L1-WT) (B), while predominantly small round mitochondria are seen in neurites of L1-deficient neurons (L1−/y) (A), in mock-transduced L1-lacking HEK293 cells (ctrl) and in HEK293 cells expressing the L1 mutant (L1-R/A) (B). (C) HEK293 cells transduced with control AAV or with AAV coding for wild-type L1 or L1 mutant and transfected with the photo-convertible fluorescent mitochondrial protein Mito-Dendra-2 are exposed to a spot of UV light to induce the conversion of the Mito-Dendra-2 fluorescence from green to red. Representative images are shown from two independent experiments. (D) Quantifications of yellow-labeled fused mitochondria from three videos per group and experiment are shown. Fusion of mitochondria is impaired in cells not expressing L1 or expressing the L1 mutant. Mean±s.e.m. values from two independent experiments are shown (***$P<0.001$; one-way ANOVA with Holm–Sidak multiple comparison test). Scale bars: 20 µm (A), 10 µm (B,C).

impaired low membrane potential move predominantly retrogradely (Miller and Sheetz, 2004), the direction of movement was measured in wild-type and L1-deficient cerebellar neurons at 3 days of culture. At this stage, cerebellar neurons have an elaborated axon, but no dendrites, and thus only movement of mitochondria in axons was determined. In comparison to mitochondria in wild-type neurons, mitochondria in L1-deficient neurons were decreased in anterograde axonal movement and increased in retrograde axonal movement (Fig. 6E). Interestingly, the mobility of mitochondria was not affected in L1- or MBP-deficient neurons or in wild-type neurons after application of L1 function-triggering antibody relative

to the mobility of mitochondria in untreated wild-type neurons (Fig. 6F).

Mitochondrial L1-70 interacts with the complex I subunit NDUFV2

To identify mitochondrial L1-binding proteins, detergent-solubilized mitochondria isolated by means of differential and gradient centrifugations were subjected to affinity chromatography via immobilization of recombinantly expressed intracellular L1 domain (L1-ICD). The recombinant intracellular CHL1 domain (CHL1-ICD) served as control. After SDS-PAGE of the eluates and
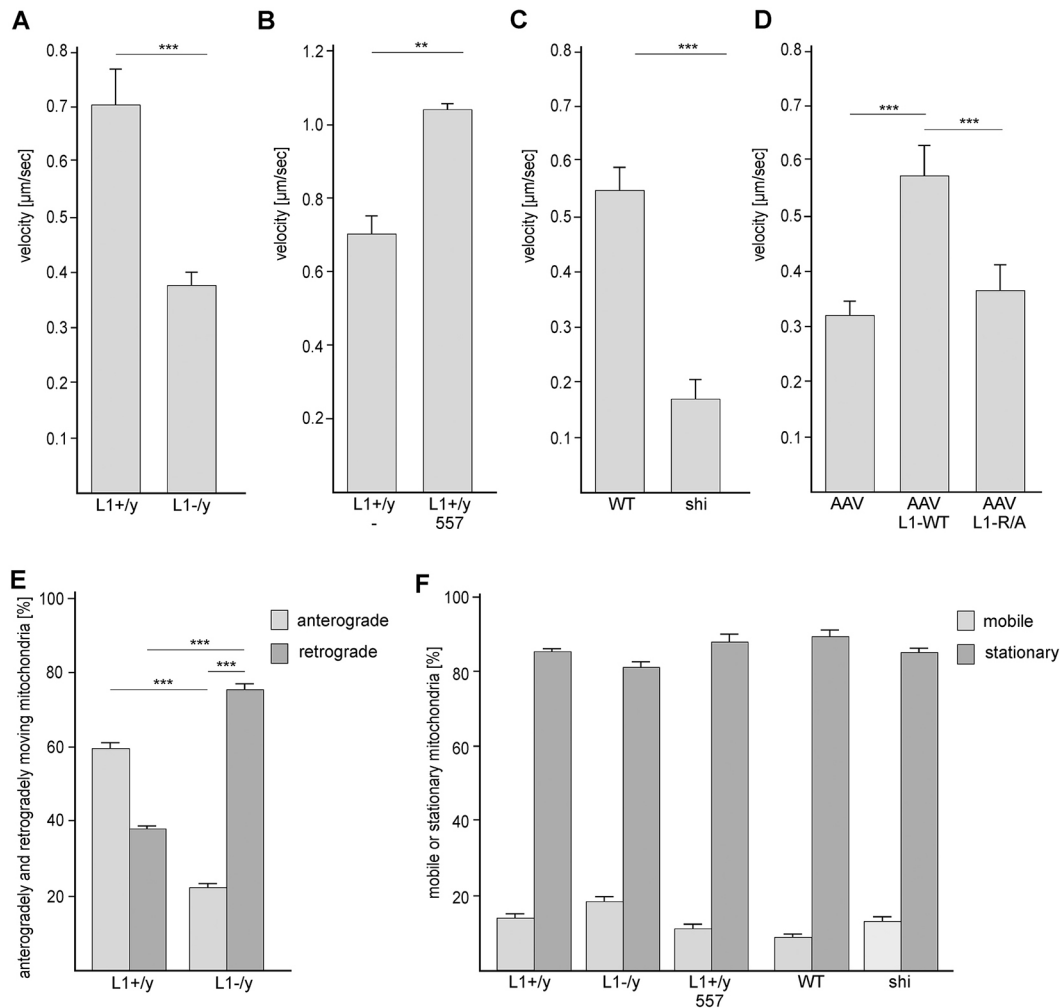
Fig. 6. Motility and directional movement of mitochondria is regulated by the absence of L1-70. Cerebellar neurons were maintained in culture for 3 days. (A) Motility of MitoTracker-labeled mitochondria is reduced in cerebellar neurons from L1-deficient mice (L1−/y) in comparison to the motility of mitochondria in neurons from corresponding wild-type littermates (L1+/y). (B) Motility of MitoTracker-labeled mitochondria is enhanced after stimulation of wild-type cerebellar neurons (L1+/y) with the function-triggering L1 antibody 557 relative to the motility of mitochondria in untreated (−) wild-type neurons. (C) Motility of MitoTracker-labeled mitochondria is reduced in L1-70-lacking neurons from MBP-deficient shiverer mice (shi) relative to corresponding wild-type littermates (WT). (D) Motility of MitoTracker-labeled mitochondria is enhanced after transduction of L1-deficient cerebellar neurons with AAV coding for wild-type L1 (AAV L1-WT), but not after transduction with control AAV or AAV coding for mutated L1 with a disrupted MBP cleavage site (AAV L1-R/A). (E) The percentage of anterogradely moving MitoTracker-labeled mitochondria is higher in wild-type than in L1-deficient cerebellar neurons, while the percentage of retrogradely moving MitoTracker-labeled mitochondria is higher in L1-deficient than in wild-type cerebellar neurons. (F) The numbers of mobile and stationary MitoTracker-labeled mitochondria are similar in non-treated L1-deficient (L1−/y), non-treated wild-type (L1+/y) and L1 antibody-treated wild-type (L1+/y 557) neurons, as well as in neurons from shiverer mice (shi) and their littermates (WT). In A–F, the motility of mobile mitochondria, percentage of mobile and stationary mitochondria, and direction of mitochondrial transport were quantified by analysis of kymographs of 50 mitochondria in 5–10 neurons per group and experiment. Mean±s.e.m. values from two experiments are shown (**$P<0.01$; ***$P<0.001$; two-tailed Student's t-test).

Coomassie Brilliant Blue staining, regions with stained bands seen in the L1-ICD eluate, but not in the CHL1-ICD eluate were cut out and analyzed by mass spectrometry. Corresponding regions in the CHL1-ICD eluate were excised and used as controls for mass spectrometry. We identified a large number of proteins which were found exclusively or predominantly in the L1-ICD eluate relative to the CHL1-ICD eluate (Tables S1, S2 and S3), suggesting that the identified proteins represent potential L1-specific binding partners. More than 50% of the proteins could be annotated to mitochondria (Fig. S1) and, interestingly, among these potential mitochondrial L1-binding proteins, we found 17 subunits out of 43 subunits of complex I (Tables S1, S2 and S3). In the 25–35 kDa band region, tryptic peptides with masses matching those of the ~27 kDa complex I subunit NDUFV2 were identified in the L1-ICD eluate,

but not in the CHL1-ICD eluate. This complex I subunit was considered to be the prime candidate for a direct interaction with L1-ICD (Table S1). A direct interaction of L1-ICD with NDUFV2 was confirmed by ELISA (Fig. 7A). Furthermore, L1-70 was co-immunoprecipitated by anti-NDUFV2 antibody from mitochondrial lysates of wild-type, but not L1-deficient mice. L1-70 was only weakly detectable when a non-immune control antibody was used for immunoprecipitation (Fig. 7B). These results indicate that L1-70 directly interacts with NDUFV2 and suggest that this interaction regulates complex I activity inside of mitochondria.

In the 75–100 kDa band region of the L1-ICD eluate, but not CHL1-ICD eluate, tryptic peptides were found to match peptides of the ~81 kDa Ras homolog family member T1 (RhoT1; also known as mitochondrial Rho GTPase 1 or MIRO1) or of the ~78 kDa
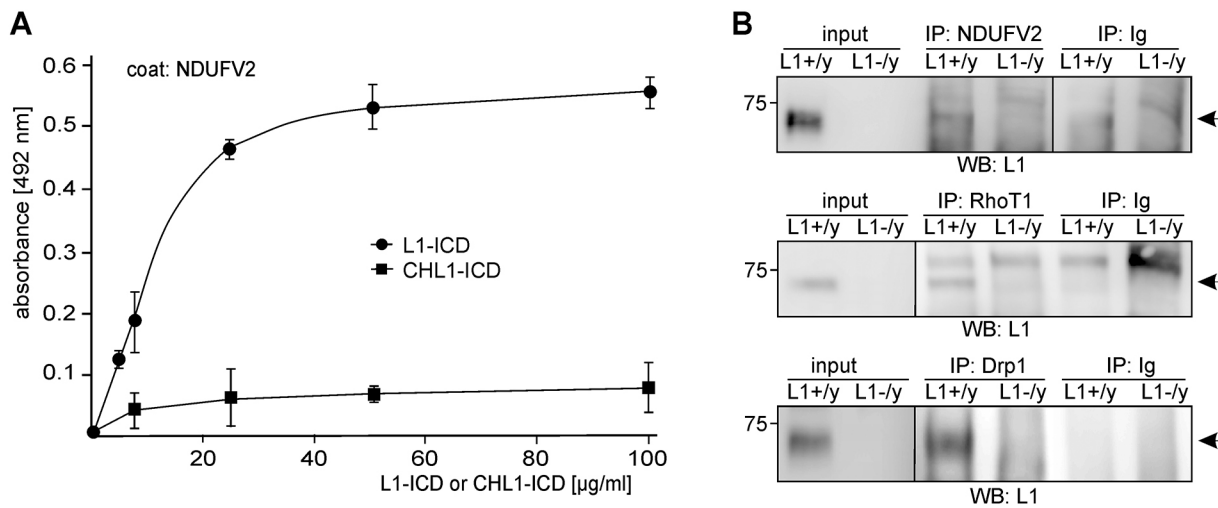
Fig. 7. Mitochondrial L1-70 interacts with NDUFV2, RhoT1 and Drp1. (A) ELISA was performed using recombinant NDUFV2 as a substrate coat and increasing concentrations of intracellular domains of L1 (L-ICD) or CHL1 (CHL1-ICD). Mean±s.e.m. values from three independent experiments carried out in triplicates are shown. (B) Mitochondrial lysates from L1-deficient mice (L1−/y) and wild-type (L1+/y) littermates were subjected to immunoprecipitation (IP) with antibodies against NDUFV2, RhoT1 or Drp1, and western blot analysis with the polyclonal rabbit anti-L1 antibody. Representative blots out of three independent experiments are shown and L1-70 is indicated by an arrow. Lanes not adjacent to each other but derived from the same blot are indicated by a vertical line.

dynamin 1-like protein (Dnm1l; also known as dynamin-related protein 1 or Drp1). Since RhoT1 contributes to mitochondrial fission and since Drp1 plays a crucial role in mitochondrial trafficking, we investigated whether these proteins interact with L1-70.

L1-70 was co-immunoprecipitated with anti-RhoT1 and anti-Drp1 antibody, but not by control antibodies, from mitochondrial lysates of wild-type but not L1-deficient mice (Fig. 7B). These results suggest that L1-70 interacts with RhoT1 and Drp1 at the outer surface of mitochondria and that these interactions contribute to mitochondrial movement and fission–fusion cycles.

DISCUSSION

In the present study, we show that L1-70 is imported into mitochondria, where it interacts with the complex I subunit NDUFV2 and regulates its activity. The import of L1-70 is blocked by anti-TOM70 antibody, indicating that L1-70, which has no cleavable MTS, is recognized by TOM70 and imported from the cytoplasm to the intermembrane space via the TOM complex. Given that L1-70 interacts with complex I in the mitochondrial matrix, L1-70 has to be transported from the intermembrane space to the matrix. We propose that the TOM complex mediates this transport. It is conceivable that L1-70 directly binds to TOM70 and thus initiates its import via the TOM complex. On the other hand, it is also possible that the interaction of L1-70 with TOM70 is indirect and requires cytoplasmic and/or mitochondrial proteins. It is noteworthy in this context that mitochondrial import of proteins with internal signal sequences via TOM70 requires several cytoplasmic factors, such as members of the molecular chaperone Hsc70/Hsp70 and Hsp90 families, which interact with TOM70 and mediate initiation of the import process in association with co-chaperones (for a review, see Fan and Young, 2011).

Complex I has an L-shaped structure with a hydrophobic arm located in the mitochondrial inner membrane and a hydrophilic arm protruding into the mitochondrial matrix. The membrane arm contains the proton translocation module (P module), while the peripheral arm consists of the electron input module (N module) and the electron output module (Q module). The N module contains the NADH oxidation site with flavin mononucleotide being the electron acceptor. The Q module contains the ubiquinone reduction site.

NDUFV2 is part of the N module. Since L1-70 interacts with NDUFV2, we propose that this interaction is crucial for the oxidation of NADH by the N module of complex I, which has been implicated in a multitude of neural and non-neural diseases (Mimaki et al., 2012). Impaired NADH oxidation in the absence of L1-70 may reduce the complex I-mediated transfer of protons from the matrix into the intermembrane space and may thus lead to impairment of the proton gradient and of the mitochondrial membrane potential. Since cell survival of L1-deficient cerebellar neurons under physiological conditions is similar to that of wild-type neurons (Loers et al., 2005; Lutz et al., 2014a), we exclude the possibility that the reduction of mitochondrial membrane potential in L1-deficient neurons is due to increased apoptosis.

L1-70 contains the third, fourth and fifth fibronectin type III homologous repeats that are part of the extracellular L1 domain and mediate L1 autophosphorylation. These repeats contain sequences that resemble the Rossmann motif GxGxxG, and a sequence motif found in GAPDH and in the catalytic domain of almost all of the known serine, threonine and tyrosine protein kinases (Makhina et al., 2009). The Rossmann motif is part of the Rossmann fold, which is present in proteins that bind nucleotides, such as enzyme cofactors FMN, FAD, and NAD as well as ATP. In addition to the GxGxxG motif, other motifs, such as GxGxxP, GxxxG/A and RxS/T (Dym and Eisenberg, 2001; Kleiger and Eisenberg, 2002; Roma et al., 2005), are involved in binding of NADH, NADPH, FAD or FMN. Interestingly, two GxGxxG motifs (G_{794}KGPEP, G_{899}RGSGP), five GxxxG motifs (G_{842}HLRG, G_{899}RGSG G_{946}VLTG, G_{1223}SFIG, G_{1227}QYSG), five GxxxA motifs (G_{918}HPEA, G_{1000}PGEA, G_{1009}GTMA, G_{1021}NISA, G_{1124}FVSA) and one RxYS motif (R_{885}PYS) are present in L1-70, suggesting that L1-70 binds to nucleotides, such as NADH. Thus, it is conceivable that binding of NADH and other nucleotides, for example, ATP, and/or the kinase activity of L1 contributes to the effect of L1 on complex I activity. Since GAPDH produces NADH via oxidative phosphorylation and L1 binds to GAPDH via its third, fourth and/or fifth fibronectin type III homologous repeats (Makhina et al., 2009), it is possible that the interaction of L1 with GAPDH enhances the GAPDH activity and, thus, the NADH levels generated by GAPDH. Lack of L1-70 could lead to reduced

production of NADH, thus contributing to the impaired generation of an intact mitochondrial membrane potential.

We showed that the impaired mitochondrial membrane potential, which is associated with reduced mitochondrial motility, impairs mitochondrial fusion/fission and enhances retrograde transport of mitochondria. We assume that the reduced mitochondrial membrane potential in the absence of L1-70 causes the alterations in mitochondrial dynamics, because an intact mitochondrial membrane potential is essential for the fusion and movement of mitochondria (for a review, see Oliveira, 2011). L1-70 interacts with RhoT1, which is involved in mitochondrial trafficking and control of anterograde transport of mitochondria. It also interacts with Drp1, which is important for mitochondrial fission. Thus, it is likely that the interaction of L1-70 with RhoT1 and Drp1 at the outer surface of mitochondria leads to enhancement of motility and to reduction of fission, and that lack of L1-70 reduces motility and enhances fission and fragmentation, thereby decreasing the fusion of mitochondria.

Impairments of mitochondrial functions cause neurodegeneration, notably in the development of disorders, such as, for instance, Huntington's, Alzheimer's and Parkinson's diseases (for reviews, see Chen and Chan, 2009; Golpich et al., 2017). It is noteworthy in this context that L1-70 levels are reduced in a mouse model of Alzheimer's disease, and L1 overexpression is protective for neurons in this mouse model (Lutz et al., 2012; Djogo et al., 2013). L1 mutations are associated with neural disorders, such as schizophrenia, Alzheimer's disease and the L1 syndrome, which is characterized by hydrocephalus, cognitive disability and motor dysfunctions (Poltorak et al., 1995; Kurumaji et al., 2001; Strekalova et al., 2006; Wakabayashi et al., 2008; for reviews, see Maness and Schachner, 2007; Schäfer and Altevogt, 2010). Interestingly, NDUFV2 has been linked to Parkinson's and Alzheimer's diseases, bipolar disorder, schizophrenia and encephalopathy, and Drp1 has been implicated in several neurological disorders, including Alzheimer's disease. Based on these findings, it is tempting to speculate that impairments of the function of L1-70 in mitochondria and disturbance of the interactions of L1-70 with NDUFV2, and most likely also with Drp1, contribute to the development of degenerative diseases not only in the nervous system, but also in other organs. These diseases will become more frequent in increasingly aging populations.

MATERIALS AND METHODS
Animals
L1-deficient mice (Dahme et al., 1997), CHL1-deficient mice (Montag-Sallaz et al., 2002), NCAM-deficient mice (Cremer et al., 1994) and MBP-deficient shiverer mice (Wolf and Billings-Gagliardi, 1984; Mikoshiba et al., 1983) were maintained as heterozygous breeding pairs. L1-deficient mice were maintained on a mixed genetic background (129SVJ×C57BL/6×Black Swiss), and CHL1-, NCAM- and MBP-deficient mice were maintained on an inbred C57BL/6J background. Wild-type littermates of either sex were used as controls in experiments where CHL1-, NCAM- and MBP-deficient mice of either sex were investigated, and wild-type male littermates were used for experiments with L1-deficient males. C57BL/6J mice were used as wild-type mice in all other experiments. Mice were maintained under standard laboratory conditions with food and water supply *ad libitum* and with a 12-h-light–12-h-dark cycle. All experiments were conducted in accordance with the German and European Community laws on protection of experimental animals and were approved by the responsible committee of The State of Hamburg.

Antibodies and reagents
The monoclonal mouse anti-L1 CD171 antibody, recognizing an epitope close to amino acid 1172 of chick L1 (clone 74-5H7; Cat #38101; lot B222192), was from BioLegend (San Diego, CA) and used at a 1:200 dilution. The polyclonal rabbit anti-L1 antibody L1CAM against amino acids

1153–1182 of human L1 (ab123990; lot GR104917-13) and the donkey anti-rabbit-IgG antibody conjugated to 5 nm colloidal gold were from Abcam (Cambridge, UK) and used at a 1:1000 and 1:200 dilution, respectively. The anti-L1 antibodies recognizing an epitope at amino acids 921–1120 (H-200; sc-15326; lot K1804) or in the intracellular domain of human L1 (C-2; sc-514360; lot: E1517) and the antibodies against GAPDH (FL-335; sc-25778; lot D1613), TOM70 (H-117; sc-366282; lot G2514), NDUFV2 (F-5; sc-271620; lot L0211), NDUFV3 (D-16; sc-83307; lot G2415), calreticulin (calregulin; T-70; sc-7431; lot C1806), VDAC1 (B-6; sc-390996; lot J0517), EEA1 (G-4;sc-137130; lot J0317), Rab7 (B-3; sc-376362; lot G3117) and histone H3(C-16; sc-8654; lot I2013) were from Santa Cruz Biotechnology (Heidelberg, Germany) and used at a 1:500 dilution. Anti-RhoA antibody (ARH04; clone 7F1.E5) was from Cytoskeleton (Denver, CO) and used at a 1:1000 dilution. Non-immune control antibodies, non-immune goat serum and secondary antibodies coupled to horseradish peroxidase (HRP) (1:20,000) or conjugated to fluorescent dyes (1:200) were purchased from Dianova (Hamburg, Germany). Recombinant full-length human NDUFV2 (H00004729-P01) was from Abnova (Taipei, Taiwan). Cloning and production of recombinant His-tagged intracellular L1 or CHL1 domains have been described previously (Xiao et al., 2009). MitoTracker (MitoTracker® Red CMXRos; M-7512) was from ThermoFisher Scientific (Darmstadt, Germany). The MitoDendra-2 plasmid (plasmid #55796) was from Addgene (deposited by David Chan; Pham et al., 2012).

Isolation of mitochondria and determination of complex I, II/III, IV and V activities
For the isolation of mitochondria from brain tissue, the Mitochondria Isolation Kit for Tissue (#89801) from ThermoFisher Scientific was used. For determination of the complex I–V activities, mitochondria were applied to the Mitochondrial Complex I Activity Assay Kit (AAMT001) from Merck Chemicals (Millipore; Schwalbach, Germany) and to the MitoCheck Complex II/III Activity Assay Kit (Cay-700950), the MitoCheck Complex IV Activity Assay Kit (Cay700990-96) or the MitoCheck Complex V Activity Assay Kit (Cay-701000-96) from Biomol (Hamburg, Germany).

AAV-transduction of HEK293 cells and cultured cerebellar neurons
Site-directed mutagenesis of R_{687} to A_{687} (L1R/A) has been described previously (Lutz et al., 2014a). Subcloning of wild-type and mutated L1 into pAAV-MCS vector and production of AAV that encodes wild-type and mutated L1 was performed as described previously (Lutz et al., 2014a). For viral transduction, AAV1 carrying wild-type and mutant L1 were incubated for 24 h at a 1000-fold multiplicity of infection with L1-deficient cerebellar neurons or HEK293 cells. Cultures of HEK293 cells (ATCC CRL-1573™; authentication and testing for contamination every 3 months) or cerebellar neurons were prepared and maintained as described previously (Kleene et al., 2010). For time-lapse video microscopy and kymographic analysis, cerebellar neurons were maintained in culture for 3 days.

Western analysis and immunoprecipitation
Immunoblot analysis and immunoprecipitation was performed as described previously (Makhina et al., 2009).

ELISA
Recombinant NDUFV2 (25 µl of 5 µg/ml per well) in Dulbecco's phosphate-buffered saline with Ca^{2+} and Mg^{2+} (PBS^{2+}) (Sigma-Aldrich, Taufkirchen, Germany) was coated overnight in a 384-well high-binding polystyrene plate (Corning, Tewksbury, MA) at 4°C. The following steps were performed at room temperature. After washing the wells with PBS^{2+}, blocking with 2% essentially fatty acid-free bovine serum albumin (BSA) (Sigma-Aldrich) in PBS^{2+} for 1 h and washing with PBS^{2+}, the recombinant intracellular domains of L1 or CHL1 (10 µl of 0, 6.25, 12.5, 25, 50 or 100 µg/ml per well) were added and incubated for 1 h. After washing once with PBS^{2+} and twice with PBS-T (PBS^{2+} supplemented with 0.05% Tween 20) the polyclonal rabbit anti-L1 antibody L1CAM (diluted 1:100 in PBS^{2+}) was added and incubated for 1 h. After three washes with PBS-T, HRP-coupled anti-mouse-IgG secondary antibody (diluted 1:2000 in PBS^{2+}) was

added and incubated for 1 h. After two washes with PBS^{2+} and three washes with PBS-T, o-phenylenediamine dihydrochloride (Thermo Scientifc) was added at a concentration of 1 mg/ml. The color reaction was terminated with 2.4 M sulfuric acid, and absorbance was measured at 492 nm using the μQuant^{TM} microplate spectrophotometer.

Subcellular fractionation and *in vitro* import assay

For the isolation of cytoplasmic fractions, brains from 4-week-old wild-type mice were homogenized in Dulbecco's phosphate-buffered saline without Ca^{2+} and Mg^{2+} (PBS) and centrifuged at 1000 *g* for 10 min at 4°C. The supernatants were centrifuged at 17,000 *g* for 20 min at 4°C and thereafter centrifuged at 100,000 *g* for 45 min at 4°C. The resulting supernatants were used as the cytoplasmic fraction. The 100,000 *g* pellet was used as the microsomal fraction enriched in endosomes and endoplasmic reticulum. Nuclei were isolated as described previously (Lutz et al., 2012). Mitochondria were isolated from brains of 4-week-old L1-deficient mice using the Mitochondria Isolation Kit for Tissue. Cytoplasmic fractions and mitochondria were incubated at 37°C under constant agitation for 1 h in the absence or presence of anti-TOM70 antibody, anti-L1 antibody H-200 or non-immune control antibodies (30 μg/ml). The samples were then centrifuged at 12,000 *g* for 10 min at 4°C. The pellets were resuspended in PBS and treated or not treated with 0.05% trypsin and 0.02% EDTA (Sigma-Aldrich) (diluted 1:5 in PBS without Ca^{2+} and Mg^{2+}) in the absence or presence of 1% Triton X-100 for 5 min at room temperature followed by incubation with 1 mg/ml trypsin inhibitor for 5 min at room temperature. The samples that were not incubated with Triton X-100 were centrifuged at 12,000 *g* and 4°C for 10 min, and the resulting pellet was resuspended in mitochondrial lysis buffer (20 mM Tris-HCl pH 7.5, 150 mM NaCl, 1 mM EDTA, 1 mM EGTA, 1% NP-40, 1% sodium deoxycholate, 2.5 mM sodium pyrophosphate, 1 mM β-glycerophosphate and 1 mM sodium vanadate) containing protease inhibitor cocktail (Roche Diagnostics). The samples were then centrifuged at 12,000 *g* and 4°C for 10 min, and the resulting supernatants and the samples treated with Triton X-100 were subjected to methanol/chloroform protein precipitation.

Pre-embedding immunogold labeling and electron microscopy

Animals were anesthetized with sodium pentobarbital and perfused transcardially with physiological saline followed by fixative solution containing 0.5% glutaraldehyde and 4% formaldehyde in 0.1 M phosphate buffer, pH 7.4. Cerebella were then removed and stored in fixative solution at 4°C overnight, washed in phosphate buffer and sectioned sagittally on a vibratome (Leica VT 10005) at a thickness of 50 μm. Sections were incubated in blocking solution containing 5% non-immune goat serum in phosphate buffer for 30 min, then incubated with rabbit mouse anti-L1 antibody H-200 at room temperature overnight, followed by washing in phosphate buffer for 30 min and incubation with anti-rabbit immunoglobulin antibody conjugated to 5 nm colloidal gold (diluted 1:200) for 2 h. After washing in phosphate buffer for 30 min, sections were fixed in 2% aqueous glutaraldehyde solution for 2 min and rinsed in distilled water for 10 min. Osmication, dehydration, embedding in Epon, ultrathin sectioning and electron microscopy were performed as described previously (Westphal et al., 2016).

Determination of the mitochondrial membrane potential

For determination of the membrane potential MITO-ID® Membrane potential detection kit (ENZ-51018-0025) from Enzo (Exeter, UK) was used. The green fluorescent membrane potential reagent MITO-ID accumulates as orange-fluorescent aggregates in mitochondria with intact membrane potential. To quantify the membrane potential, the level of the fluorescence intensity in a given region of a green or orange channel was analyzed by live imaging for 10 min. The corrected total cell fluorescence (CTCF) was calculated with the ImageJ software using the formula CTCF=integrated density−(area of selected cell×mean fluorescence of background readings) (McCloy et al., 2014).

Transient transfection of HEK293 cells

HEK293 cells were seeded at a density of 10^6 cells/ml on poly-L-lysine-coated glass coverslips and maintained until they reached a density of 70–90%. For transfection, 6 μl of Lipofectamine® LTX Reagent (ThermoFisher

Scientific) was mixed with serum-free DMEM, incubated for 5 min, then mixed with 5 μg of the MitoDendra-2 plasmid and 4 μl of PLUS™ Reagent (ThermoFisher Scientific). The mixture was incubated for 30 min at room temperature and applied to the culture medium. Cells were maintained for 3 days at 37°C, 5% CO$_2$ and 90% relative humidity.

Determination of fission/fusion

For determination of mitochondrial morphology, cells were incubated in medium containing 100 nM MitoTracker for 30 min at 37°C. Cells were then subjected to fixation in 4% formaldehyde for 20 min at room temperature. Fixed cells were washed once in PBS without Ca^{2+} and Mg^{2+} and mounted in Roti-Mount® containing DAPI for staining of nuclei. For determination of fusion, cells were transfected with MitoDendra-2 plasmid. Positively transfected cells were chosen and images in the green and red channel were taken every 2 s for 5 min before and after photobleaching of a defined region of interest (ROI) using a 405 nm laser at 2% intensity. Images were analyzed with the ImageJ software to determine the area occupied by fused mitochondria in the defined ROI.

Microscopy

Fluorescence imaging was performed using the Olympus FluoView TMFV1000 (Olympus, Hamburg, Germany) laser-scanning confocal microscope with a 60× objective. For simultaneous double-channel fluorescence, images were taken in a sequential scanning mode. Images were adjusted for brightness and contrast using Adobe Photoshop CS5 software (Adobe Systems, San José, CA).

Time-lapse video microscopy and kymographic analysis

For labeling of mitochondria, cells were incubated in medium containing 100 nM MitoTracker for 30 min at 37°C. The staining solution was replaced by fresh medium, and the cells were analyzed by time-lapse imaging using an upright microscope (Nikon Instruments, Amsterdam, The Netherlands) combined with spinning disc (Yokogawa, Hamburg, Germany) live-cell confocal technology (Visitron Systems, Puchheim, Germany) and a 60× objective. For single-channel live imaging, a 561 nm laser was used, and images were taken at intervals of 2 s for a duration of 5 min. Videos were acquired using the VisiView software (Visitron Systems).

To determine mitochondrial motility, and the mobility and the direction of the mitochondrial transport (anterograde or retrograde), the kymograph (time space plot) plugin and the velocity tool from ImageJ (https://www.embl.de/eamnet/html/body_kymograph.html; ImageJ Kymograph Analysis handout, Rietdorf and Seitz, 2008, Heidelberg: Homepage of European Advanced Light Microscopy Network) was used. The kymograph represents a time and space plot: the *x*-axis indicates the distance and the *y*-axis shows the time. Vertical lines represent no movement, while diagonal lines show mobile mitochondria. Depending on the position of the cell soma, the direction (right or left) of diagonal lines indicate retrograde or anterograde transport (Marra et al., 2015).

Affinity chromatography and mass spectrometry

Brains from 40 4-month-old wild-type mice were homogenized in 80 ml MIB (0.32 M sucrose, 10 mM Tris-HCl, pH 7.4, 1 mM EDTA, 1× protease inhibitor solution) using a Potter Elvehjem homogenizer. This and all following steps were performed on ice or at 4°C. The homogenate was centrifuged at 1000 *g* for 5 min and the pellet was washed twice with 12 ml MIB at 1000 *g* for 5 min. The collected supernatants were pooled and centrifuged at 1000 *g* for 5 min, followed by centrifugation of the resulting supernatant at 14,000 *g* for 15 min. The 14,000 *g* pellet was resuspended in 12 ml MIB and layered on a gradient containing 12 ml of 12% Ficoll and 12 ml of 7.5% Ficoll. The gradient was centrifuged at 73,000 *g* for 36 min. The resulting pellet containing mitochondria was resuspended in 12 ml MIB with 0.5 mg/ml BSA and centrifuged at 12,000 *g* for 15 min. The pellet containing the mitochondria was resuspended in 6 ml MIB and applied onto a gradient containing 6 ml of 0.8 M, 6 ml of 1.0 M, 10 ml of 1.3 M and 8 ml of 1.6 M sucrose. The sucrose gradient was centrifuged at 50,000 *g* for 2 h. Purified mitochondria were collected from the 1.3 M–1.6 M sucrose interface, diluted 1:3 in TE buffer (10 mM Tris-HCl pH 7.4, 1 mM EDTA, 0.5 mg/ml BSA) and centrifuged at 18,000 *g* for 15 min. The pellet

was washed twice with MIB at 12,000 g for 10 min and then 8200 g for 10 min. The pellets were washed in PBS without Ca^{2+} and Mg^{2+} at 8200 g for 10 min, resuspended and incubated in mitochondrial lysis buffer containing protease inhibitor cocktail. The intracellular domains of L1 or CHL1 were immobilized onto cyanogen bromide-activated Sepharose beads (GE Healthcare, Freiburg, Germany) according to the manufacturer's instruction. The beads were washed several times with PBS without Ca^{2+} and Mg^{2+}, 1% CHAPS in PBS without Ca^{2+} and Mg^{2+}, and PBS without Ca^{2+} and Mg^{2+} and then incubated overnight with the mitochondrial lysate. Bound proteins were eluted with 0.1 M glycine, pH 2.3, neutralized with 1 M Tris-HCl, pH 8.0, and subjected to protein precipitation. After separation of the proteins by SDS-PAGE and staining with Coomassie Brilliant Blue, visible bands were excised and subjected to mass spectrometry (LC-MS/MS). LC-MS/MS was performed by Peter Lobel and Haiyan Zheng (Rutgers Mass Spectrometry Center for Integrative Neuroscience Research, Piscataway, NJ, USA).

Supplementary information
Supplementary information available online at
http://jcs.biologists.org/lookup/doi/10.1242/jcs.210500.supplemental

References
Anderson, R. B., Turner, K. N., Nikonenko, A. G., Hemperly, J., Schachner, M. and Young, H. M. (2006). The cell adhesion molecule L1 is required for chain migration of neural crest cells in the developing mouse gut. *Gastroenterology* **130**, 1221-1232.

Barbin, G., Aigrot, M. S., Charles, P., Foucher, A., Grumet, M., Schachner, M., Zalc, B. and Lubetzki, C. (2004). Axonal cell-adhesion molecule L1 in CNS myelination. *Neuron Glia Biol.* **1**, 65-72.

Becker, T., Böttinger, L. and Pfanner, N. (2012). Mitochondrial protein import: from transport pathways to an integrated network. *Trends Biochem. Sci.* **37**, 85-91.

Chen, H. and Chan, D. C. (2009). Mitochondrial dynamics - fusion, fission, movement, and mitophagy - in neurodegenerative diseases. *Hum. Mol. Genet.* **18**, R169-R176.

Chen, J., Wu, J., Apostolova, I., Skup, M., Irintchev, A., Kügler, S. and Schachner, M. (2007). Adeno-associated virus-mediated L1 expression promotes functional recovery after spinal cord injury. *Brain* **130**, 954-969.

Cremer, H., Lange, R., Christoph, A., Plomann, M., Vopper, G., Roes, J., Brown, R., Baldwin, S., Kraemer, P., Scheff, S. et al. (1994). Inactivation of the N-CAM gene in mice results in size reduction of the olfactory bulb and deficits in spatial learning. *Nature* **367**, 455-459.

Cui, Y.-F., Xu, J.-C., Hargus, G., Jakovcevski, I., Schachner, M. and Bernreuther, C. (2011). Embryonic stem cell-derived L1 overexpressing neural aggregates enhance recovery after spinal cord injury in mice. *PLoS One* **6**, e17126.

Dahme, M., Bartsch, U., Martini, R., Anliker, B., Schachner, M. and Mantei, N. (1997). Disruption of the mouse L1 gene leads to malformations of the nervous system. *Nat. Genet.* **17**, 346-349.

Debiec, H., Kutsche, M., Schachner, M. and Ronco, P. (2002). Abnormal renal phenotype in L1 knockout mice: a novel cause of CAKUT. *Nephrol. Dial. Transplant.* **17**(Suppl 9), 42-44.

Djogo, N., Jakovcevski, I., Müller, C., Lee, H. J., Xu, J.-C., Jakovcevski, M., Kügler, S., Loers, G. and Schachner, M. (2013). Adhesion molecule L1 binds to amyloid beta and reduces Alzheimer's disease pathology in mice. *Neurobiol. Dis.* **56**, 104-115.

Dym, O. and Eisenberg, D. (2001). Sequence-structure analysis of FAD-containing proteins. *Protein Sci.* **10**, 1712-1728.

Endo, T. and Yamano, K. (2010). Transport of proteins across or into the mitochondrial outer membrane. *Biochim. Biophys. Acta* **1803**, 706-714.

Fan, A. C. and Young, J. C. (2011). Function of cytosolic chaperones in Tom70-mediated mitochondrial import. *Protein Pept. Lett.* **18**, 122-131.

Ferramosca, A. and Zara, V. (2013). Biogenesis of mitochondrial carrier proteins: molecular mechanisms of import into mitochondria. *Biochim. Biophys. Acta* **1833**, 494-502.

Golpich, M., Amini, E., Mohamed, Z., Azman Ali, R., Mohamed Ibrahim, N. and Ahmadiani, A. (2017). Mitochondrial dysfunction and biogenesis in neurodegenerative diseases: pathogenesis and treatment. *CNS Neurosci. Ther.* **23**, 5-22.

Hortsch, M. (2000). Structural and functional evolution of the L1 family: are four adhesion molecules better than one? *Mol. Cell. Neurosci.* **15**, 1-10.

Hortsch, M., Nagaraj, K. and Mualla, R. (2014). The L1 family of cell adhesion molecules: a sickening number of mutations and protein functions. *Adv. Neurobiol.* **8**, 195-229.

Kleene, R., Mzoughi, M., Joshi, G., Kalus, I., Bormann, U., Schulze, C., Xiao, M.-F., Dityatev, A. and Schachner, M. (2010). NCAM-induced neurite outgrowth depends on binding of calmodulin to NCAM and on nuclear import of NCAM and fak fragments. *J. Neurosci.* **30**, 10784-10798.

Kleiger, G. and Eisenberg, D. (2002). GXXXG and GXXXA motifs stabilize FAD and NAD(P)-binding Rossmann folds through C(alpha)-H…O hydrogen bonds and van der waals interactions. *J. Mol. Biol.* **323**, 69-76.

Kurumaji, A., Nomoto, H., Okano, T. and Toru, M. (2001). An association study between polymorphism of L1CAM gene and schizophrenia in a Japanese sample. *Am. J. Med. Genet.* **105**, 99-104.

Kamiguchi, H., Hlavin, M. L. and Lemmon, V. (1998). Role of L1 in neural development: what the knockouts tell us. *Mol. Cell. Neurosci.* **12**, 48-55.

Lavdas, A. A., Chen, J., Papastefanaki, F., Chen, S., Schachner, M., Matsas, R. and Thomaidou, D. (2010). Schwann cells engineered to express the cell adhesion molecule L1 accelerate myelination and motor recovery after spinal cord injury. *Exp. Neurol.* **221**, 206-216.

Loers, G. and Schachner, M. (2007). Recognition molecules and neural repair. *J. Neurochem.* **101**, 865-882.

Loers, G., Chen, S., Grumet, M. and Schachner, M. (2005). Signal transduction pathways implicated in neural recognition molecule L1 triggered neuroprotection and neuritogenesis. *J. Neurochem.* **92**, 1463-1476.

Loers, G., Makhina, T., Bork, U., Dörner, A., Schachner, M. and Kleene, R. (2012). The interaction between cell adhesion molecule L1, matrix metalloproteinase 14, and adenine nucleotide translocator at the plasma membrane regulates L1-mediated neurite outgrowth of murine cerebellar neurons. *J. Neurosci.* **32**, 3917-3930.

Lutz, D., Wolters-Eisfeld, G., Joshi, G., Djogo, N., Jakovcevski, I., Schachner, M. and Kleene, R. (2012). Generation and nuclear translocation of a sumoylated transmembrane fragment of the cell adhesion molecule L1. *J. Biol. Chem.* **287**, 17161-17175.

Lutz, D., Loers, G., Kleene, R., Oezen, I., Kataria, H., Katagihallimath, N., Braren, I., Harauz, G. and Schachner, M. (2014a). Myelin basic protein cleaves cell adhesion molecule L1 and promotes neuritogenesis and cell survival. *J. Biol. Chem.* **289**, 13503-13518.

Lutz, D., Wolters-Eisfeld, G., Schachner, M. and Kleene, R. (2014b). Cathepsin E generates a sumoylated intracellular fragment of the cell adhesion molecule L1 to promote neuronal and Schwann cell migration as well as myelination. *J. Neurochem.* **128**, 713-724.

Lutz, D., Kataria, H., Kleene, R., Loers, G., Chaudhary, H., Guseva, D., Wu, B., Jakovcevski, I. and Schachner, M. (2016). Myelin basic protein cleaves cell adhesion molecule L1 and improves regeneration after injury. *Mol. Neurobiol.* **53**, 3360-3376.

Makhina, T., Loers, G., Schulze, C., Ueberle, B., Schachner, M. and Kleene, R. (2009). Extracellular GAPDH binds to L1 and enhances neurite outgrowth. *Mol. Cell. Neurosci.* **41**, 206-218.

Maness, P. F. and Schachner, M. (2007). Neural recognition molecules of the immunoglobulin superfamily: signaling transducers of axon guidance and neuronal migration. *Nat. Neurosci.* **10**, 19-26.

Marra, M. H., Tobias, Z. J., Cohen, H. R., Glover, G. and Weissman, T. A. (2015). In vivo time-lapse imaging in the zebrafish lateral line: a flexible, open-ended research project for an undergraduate neurobiology laboratory course. *J. Undergrad. Neurosci. Educ.* **13**, A215-A224.

McCloy, R. A., Rogers, S., Caldon, C. E., Lorca, T., Castro, A. and Burgess, A. (2014). Partial inhibition of Cdk1 in G 2 phase overrides the SAC and decouples mitotic events. *Cell Cycle* **13**, 1400-1412.

Mikoshiba, K., Takamatsu, K. and Tsukada, Y. (1983). Peripheral nervous system of shiverer mutant mice: developmental change of myelin components and immunohistochemical demonstration of the absence of MBP and presence of P2 protein. *Brain Res.* **283**, 71-79.

Miller, K. E. and Sheetz, M. P. (2004). Axonal mitochondrial transport and potential are correlated. *J. Cell Sci.* **117**, 2791-2804.

Mimaki, M., Wang, X., McKenzie, M., Thorburn, D. R. and Ryan, M. T. (2012). Understanding mitochondrial complex I assembly in health and disease. *Biochim. Biophys. Acta* **1817**, 851-862.

Montag-Sallaz, M., Schachner, M. and Montag, D. (2002). Misguided axonal projections, neural cell adhesion molecule 180 mRNA upregulation, and altered behavior in mice deficient for the close homolog of L1. *Mol. Cell. Biol.* **22**, 7967-7981.

Oliveira, J. M. A. (2011). Mitochondrial membrane potential and dynamics. In: *Mitochondrial Dysfunction in Neurodegenerative Disorders* (eds A. K. Reeve, K. J. Krishnan, M. R. Duchen, D. M. Turnbull), pp. 127-139. London Dordrecht Heidelberg New York: Springer.

Pham A. H., McCaffery J. M. and Chan D. C. (2012). Mouse lines with photo-activatable mitochondria to study mitochondrial dynamics. *Genesis* **50**, 833-843.

Poltorak, M., Khoja, I., Hemperly, J. J., Williams, J. R., el-Mallakh, R. and Freed, W. J. (1995). Disturbances in cell recognition molecules [N-CAM and L1 antigen] in the CSF of patients with schizophrenia. *Exp. Neurol.* **131**, 266-272.

Roonprapunt, C., Huang, W., Grill, R., Friedlander, D., Grumet, M., Chen, S., Schachner, M. and Young, W. (2003). Soluble cell adhesion molecule L1-Fc promotes locomotor recovery in rats after spinal cord injury. *J. Neurotrauma* **20**, 871-882.

Roma, G. W., Crowley, L. J., Davis, C. A. and Barber, M. J. (2005). Mutagenesis of Glycine 179 modulates both catalytic efficiency and reduced pyridine nucleotide specificity in cytochrome b5 reductase. *Biochemistry* **44**, 13467-13476.

Schäfer, M. K. E. and Altevogt, P. (2010). L1CAM malfunction in the nervous system and human carcinomas. *Cell Mol. Life Sci.* **67**, 2425-2437.

Schmid, R. S. and Maness, P. F. (2008). L1 and NCAM adhesion molecules as signaling coreceptors in neuronal migration and process outgrowth. *Curr. Opin. Neurobiol.* **18**, 245-250.

Schmidt, O., Pfanner, N. and Meisinger, C. (2010). Mitochondrial protein import: from proteomics to functional mechanisms. *Nat. Rev. Mol. Cell. Biol.* **11**, 655-667.

Strekalova, H., Buhmann, C., Kleene, R., Eggers, C., Saffell, J., Hemperly, J., Weiller, C., Müller-Thomsen, T. and Schachner, M. (2006). Elevated levels of neural recognition molecule L1 in the cerebrospinal fluid of patients with Alzheimer disease and other dementia syndromes. *Neurobiol. Aging* **27**, 1-9.

Sytnyk, V., Leshchyns'ka, I. and Schachner, M. (2017). Neural cell adhesion molecules of the immunoglobulin superfamily regulate synapse formation, maintenance, and function. *Trends Neurosci.* **40**, 295-308.

Vance, J. E. (2014). MAM (mitochondria-associated membranes) in mammalian cells: lipids and beyond. *Biochim. Biophys. Acta* **1841**, 595-609.

Wakabayashi, Y., Uchida, S., Funato, H., Matsubara, T., Watanuki, T., Otsuki, K., Fujimoto, M., Nishida, A. and Watanabe, Y. (2008). State-dependent changes in the expression levels of NCAM-140 and L1 in the peripheral blood cells of bipolar disorders, but not in the major depressive disorders. *Prog. Neuropsychopharmacol. Biol. Psychiatry* **32**, 1199-1205.

Wallace, A. S., Tan, M. X., Schachner, M. and Anderson, R. B. (2011). L1cam acts as a modifier gene for members of the endothelin signalling pathway during enteric nervous system development. *Neurogastroenterol. Motil.* **23**, e510-e522.

Westphal, N., Kleene, R., Lutz, D., Theis, T. and Schachner, M. (2016). Polysialic acid enters the cell nucleus attached to a fragment of the neural cell adhesion molecule NCAM to regulate the circadian rhythm in mouse brain. *Mol. Cell. Neurosci.* **74**, 114-127.

Wolf, M. K. and Billings-Gagliardi, S. (1984). CNS hypomyelinated mutant mice (jimpy, shiverer, quaking): in vitro evidence for primary oligodendrocyte defects. *Adv. Exp. Med. Biol.* **181**, 115-133.

Xiao, M.-F., Xu, J.-C., Tereshchenko, Y., Novak, D., Schachner, M. and Kleene, R. (2009). Neural cell adhesion molecule modulates dopaminergic signaling and behavior by regulating dopamine D2 receptor internalization. *J. Neurosci.* **29**, 14752-14763.

Xu, J.-C., Bernreuther, C., Cui, Y.-F., Jakovcevski, I., Hargus, G., Xiao, M.-F. and Schachner, M. (2011). Transplanted L1 expressing radial glia and astrocytes enhance recovery after spinal cord injury. *J. Neurotrauma* **28**, 1921-1937.